ISSN 0208-7774 TRIBOLOGIA 5/2019 p. 101–113
DOI: 10.5604/01.3001.0013.6567

Wojciech RYNIEWICZ[*], Anna M. RYNIEWICZ[**], Łukasz BOJKO[***], Beata LESZCZYŃSKA-MADEJ[****], Andrzej RYNIEWICZ[*****]

ANALYSIS OF SURFACE MICROGEOMETRY AND STRUCTURE OF LAYERED BIOMATERIALS USED FOR PROSTHETIC CONSTRUCTIONS IN DIGITAL TECHNOLOGIES

ANALIZA MIKROGEOMETRII POWIERZCHNI I STRUKTURY BIOMATERIAŁÓW WARSTWOWYCH STOSOWANYCH NA KONSTRUKCJE PROTETYCZNE W TECHNOLOGIACH CYFROWYCH

Key words: prosthetic construction, substructure, veneering layer, microgeometry, structure, roughness.

Abstract

Veneering layers of prosthetic substructures are responsible for tribological cooperation with opposite teeth in the stomatognathic system (SS). Investigations of microgeometry and structure of veneering layers are aimed at checking to what extent these layers replicate enamel parameters, which, under complex load conditions, are characterized by the phenomenon of resistance to tribological wear. Ceramic veneering layers are dedicated for substructures made in digital technologies from factory fittings by milling and laser sintering of metal powders. Using a confocal microscope, contactless tests of the surface layer stereometry were performed and surface roughness parameters were determined on samples of ceramics veneering of prosthetic substructures. The analysis was performed in comparison to the natural enamel of premolars and molars. The shaping of the surface of materials veneering the substructures is similar to the regularity determined in the statistical analysis of the enamel roughness. Layers facing samples from milling technology are characterized by lower values of roughness parameters than layers created on substructures made of SLM technology.

Słowa kluczowe: konstrukcja protetyczna, podbudowa, warstwa licująca, mikrogeometria, struktura, chropowatość.

Streszczenie

Warstwy licujące podbudowy protetyczne są odpowiedzialne za współpracę tribologiczną z zębami przeciwstawnymi w układzie stomatognatycznym (US). Badania mikrogeometrii i struktury warstw licujących mają na celu sprawdzenie, w jakim stopniu warstwy te replikują parametry szkliwa, które w złożonych warunkach obciążeń charakteryzuje się fenomenem odporności na zużycie tribologiczne. Materiałem badań są ceramiczne warstwy licujące dedykowane na podbudowy wykonane w technologiach cyfrowych: z fabrycznych kształtek metodą frezowania oraz technologią spiekania laserowego z proszków metali. Z wykorzystaniem mikroskopu konfokalnego wykonano bezstykowe badania stereometrii warstwy wierzchniej oraz wyznaczono parametry chropowatości powierzchni na próbkach ceramik licujących podbudowy protetyczne. Analizę przeprowadzono w porównaniu ze szkliwem naturalnym zębów przedtrzonowych i trzonowych. Ukształtowanie powierzchni materiałów licujących podbudowy w różnym stopniu zbliża się do regularności wyznaczonej w statystycznej analizie chropowatości szkliwa. Warstwy licujące próbki z technologii frezowania charakteryzują się niższymi wartościami parametrów chropowatości niż warstwy utworzone na podbudowach z technologii SLM.

[*] ORCID: 0000-0002-9140-198X. Jagiellonian University Medical College, Faculty of Medicine, Dental Institute, Department of Dental Prosthodontics, Montelupich 4 Street, 31-155 Cracow, Poland.

[**] ORCID: 0000-0003-2469-6527. Jagiellonian University Medical College, Faculty of Medicine, Dental Institute, Department of Dental Prosthodontics, Montelupich 4 Street, 31-155 Cracow, Poland.

[***] ORCID: 0000-0002-6024-458X. AGH University of Science and Technology, Faculty of Mechanical Engineering and Robotics, Mickiewicza 30 Ave., 30-059 Cracow, Poland.

[****] ORCID: 0000-0003-0232-9080. AGH University of Science and Technology, Faculty of Non-Ferrous Metals, Mickiewicza 30 Ave., 30-059 Cracow, Poland.

[*****] ORCID: 0000-0003-3437-7650. State University of Applied Science, Institute of Technology, Zamenhofa 1a Street, 33-300 Nowy Sącz, Poland.

INTRODUCTION

In cases of significant destruction of natural tooth crowns, when they cannot be rebuilt using conservative methods, prosthetic crowns are used for polished teeth, both with preserved living pulp and after endodontic treatment. Crowns cover the remaining tooth or serve as a fixing for more extensive permanent structures – prosthetic bridges. The bridge, apart from prosthetic crowns as fastening elements, consists of a span replacing lost teeth. Occlusion forces from the span are transferred to the teeth of the pillar teeth **(Fig. 1)**. Indications for the use of bridges limit the location of pillar teeth and the efficiency of periodontal tissues. Crowns and bridges are made in accordance with clinical procedures and with indications of strength, biocompatibility, and aesthetics **[L. 1–5]**. For prosthetic constructions metals, metal alloys, glass ceramic, or ceramic materials are used. The supporting structure of the crown or bridge, depending on the biomaterial used and the manufacturing technology, is subject to veneering. Ceramic veneering layers of the substructures are responsible for functional and tribological cooperation with opposing teeth. This topic is important because of the use of new biomaterials in modern dental prosthetics and CAD/CAM systems to design and manufacture supporting structures, which involves the need to use new procedures for their targeted veneering **[L. 3, 6–13]**.

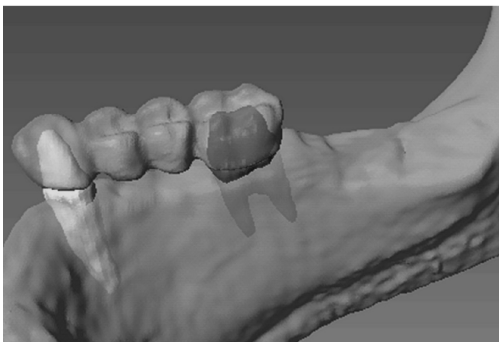

Fig. 1. Prosthetic bridge and ground crown pillars
Rys. 1. Most protetyczny i oszlifowane filary koronowe

In order for the SS to function properly, it is necessary to reproduce missing tissues in a way that is as close to natural in terms of biomechanics and biotribology as possible. The performed reconstruction should provide a physiologically similar occlusal force transfer and an adaptive wear replication. One of the most important criteria of veneering quality is the assessment of the microgeometry of the formed surface layer, which will ensure proper tribological cooperation with the enamel of natural teeth **[L. 14]**.

The aim of the study is to evaluate microgeometry and structures of layers veneering prosthetic structures produced in the technology of milling from factory blocks and in the technology of laser sintering from metal powders.

Studies on microgeometry and the structure of veneering layers will allow checking to what extent these layers reproduce the parameters of enamel, which is characterized by the phenomenon of resistance to tribological wear under complex load conditions. Inspirations for the undertaken works were a few publications comparing veneering systems dedicated to CAD/CAM methods.

MATERIAL AND METHOD

The material used in this study are complex veneering layers, dedicated for supporting substructures of crowns and bridges made in digital technologies. The procedure of creating a multilayer ceramic veneering structure depends on the type of the base material, the accuracy of its preparation, and proper execution of subsequent stages of application and firing of opaque, dentin, and enamel layers. As a result of the veneering procedure, adhesion of successive layers applied must be ensured, including adhesion to the supporting substructure under conditions of structure formation, occlusal loading, and variable temperature in the presence of saliva. In addition, aesthetic values reconstructing natural tooth tissues and proper tribological cooperation in the masticatory organ are required. The test specimen kits have been prepared in professional laboratories in accordance with the latest knowledge on innovative prosthetic construction technologies. Samples of ø1/4”, 1/16" thick circular substructures made from the following factory fittings: CoCrMo alloy, TiCP titanium, Ti6Al4V alloy, $LiSi_2$ ceramics, and ZrO_2 ceramics. Milling technology was in CAD/CAM system, and the CORiTEC 350i-imes-icore was used, 9 pieces each **(Fig. 2)**. The ZrO_2 discs were milled larger as appropriate (shrinkage factor 24%) to reach the correct structure and dimensions after sintering. Discs from supporting substructure materials made with Selective Laser Melting (SLM) method in the CAD/CAM system, 9 pieces each, were sintered from CoCrMo and Ti6Al4Vpowders on Renishaw 's AM250 **(Fig. 2)**. The discs prepared in this way, produced by milling and incremental sintering technology, were subjected to the processes of preparing the surface layer of the substructure, application of subsequent layers of dedicated ceramics and their firing **(Fig. 3)**.

After veneering with an advanced layered technique in the Dental Ceramics laboratory, research samples were subjected to analysis of microgeometry of surface and structure on the confocal microscope OLYMPUS LEXT OLS 4100. The assessment of roughness was carried out in accordance with the PN-EN ISO 4288:2011 standard. The test procedure was fully automated in a simple system for observation in reflected light. Scanning was

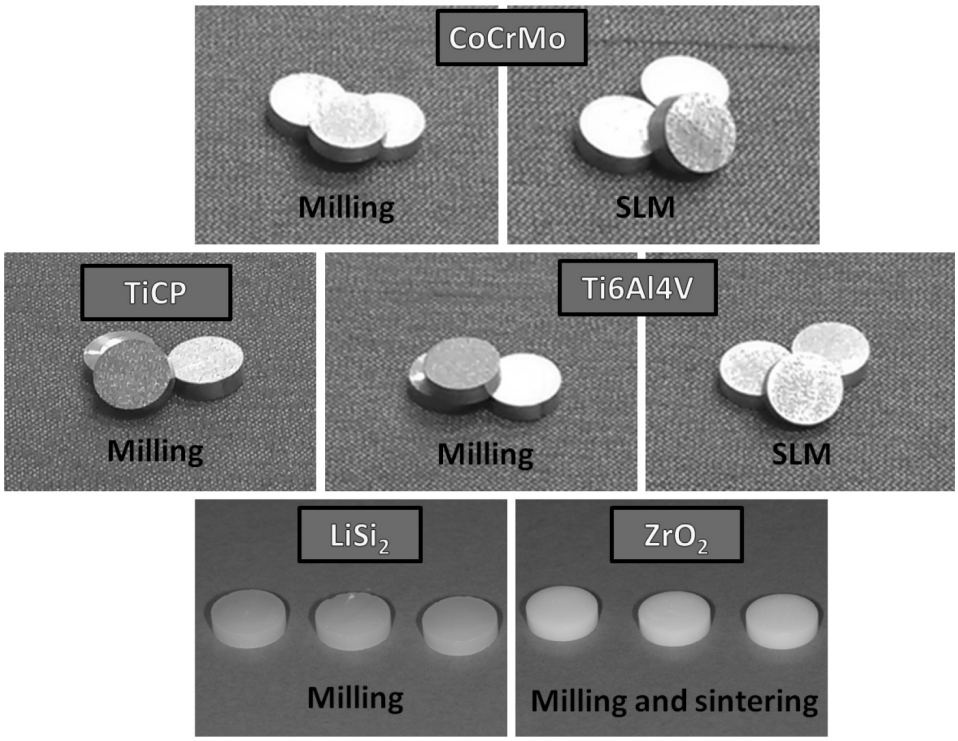

Fig. 2. Discs of material for load-bearing substructures manufactured in digital technology intended for veneering
Rys. 2. Krążki z materiałów na podbudowy nośne wytworzone w technologiach cyfrowych, przeznaczone do licowania

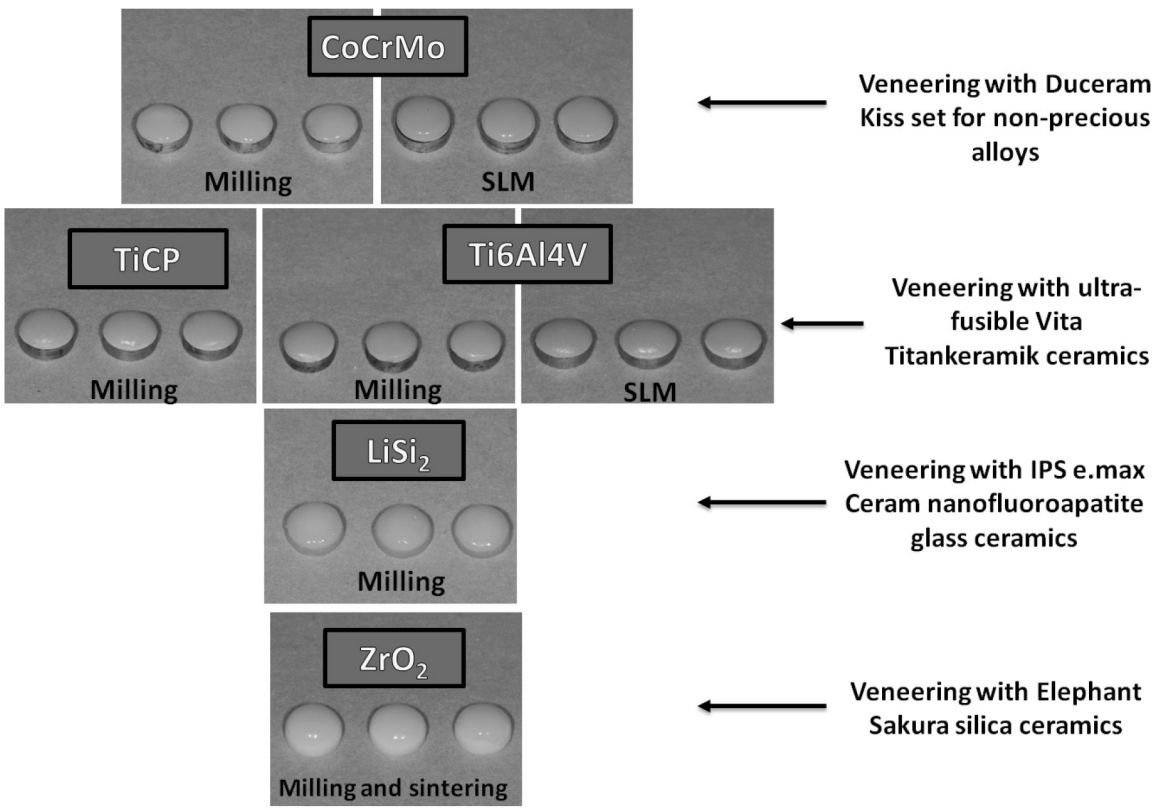

Fig. 3. Test discs with a manufactured layered veneering structure dedicated to prosthetic substructures
Rys. 3. Krążki badawcze z wytworzoną warstwową strukturą licującą dedykowaną podbudowom protetycznym

carried out on randomly selected areas with dimensions of 647 x 647 µm. The study was conducted in 3 modes: intensity 2D mode, colour 2D mode, and height mode. The reference samples were the areas of natural enamel on the surface of premolars and molars **(Fig. 4)**.

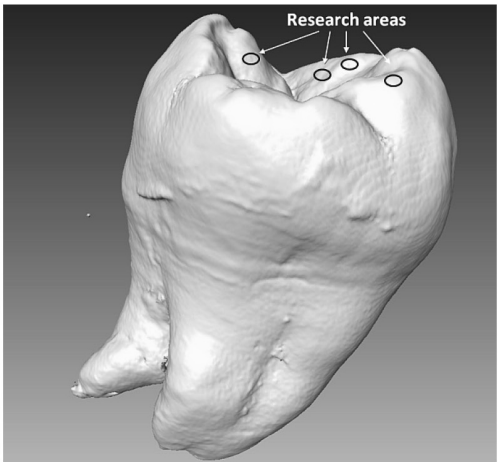

Fig. 4. A molar tooth with marked enamel test areas on the cusp surfaces. Volumetric layered reconstruction of the examined tooth based on µCT

Rys. 4. Ząb trzonowy z zaznaczonymi obszarami badawczymi szkliwa na powierzchniach guzków. Wolumetryczna rekonstrukcja warstwowa badanego zęba na podstawie µCT

PREPARATION OF TEST SAMPLES

Regardless of the application or manufacturing technique, post-firing dental ceramics consist of two phases: the vitreous phase and the crystalline phase. The vitreous phase surrounds the crystalline phase. Increasing the amount of vitreous phase reduces the resistance to cracking, but increases transparency. Full ceramic restorative materials have an increased content of crystalline phase (35–99%) in order to have better mechanical properties.

After milling and incremental sintering, the CoCrMo discs were sandblasted with Al_2O_3 with a grit size of 150 µm at a pressure of 3.5 bar. The veneering of these discs was carried out using Duceram veneering ceramics in the Kiss system. Duceram Kiss is a highly combustible dental ceramics for veneering dental alloy crowns and bridges with a coefficient of thermal expansion (CTE) of 13.8 –15.4 µm/m·K. It is characterized by an opalescence effect. The firing of ceramic layers on CoCrMo alloy discs was carried out in accordance with the procedures recommended for this type of ceramics **(Tab. 1)**.

TiCP and Ti6Al4V discs after milling and Ti6Al4V discs from incremental sintering were veneered with Vita Titankeramik ceramics. Due to the properties of titanium, such as high oxygen affinity, low thermal expansion, allotropic transformation of the crystal lattice at 882ºC, titanium creates some problems in the process of ceramic veneering. Low thermal expansion coefficient of titanium at 10 µm/m-K compared to approx. 14 µm/m-K for non-precious alloys and the α-phase transformation during cooling below 882ºC make it impossible to use conventional ceramic for titanium veneering. These properties caused the development of ceramic masses with a firing temperature below 882ºC. Ultra-low-melting ceramics with a melting point in the range of 700–850ºC were used to veneering the samples of titanium and its alloys. Preparation of titanium surfaces for connection with ceramics consisted of blast cleaning, etching, and using intermediate layers. Sandblasting with Al_2O_3 with a grit size of 250 µm at a pressure of 2–3 bar was applied. For titanium, grains with a larger diameter provide better adhesion than fine grains of the order of 50 µm. Fine grains can be pressed into the surface, which leads to a weakening of the connection with the ceramics. After sandblasting, etching was applied to clean the veneering surface and to increase its roughness. Etching has reduced the thickness of the

Table 1. Veneering parameters of Duceram Kiss ceramics on CoCrMo alloy samples after milling and incremental sintering

Tabela 1. Parametry licowania ceramiką Duceram Kiss na próbkach ze stopu CoCrMo po frezowaniu oraz ze spiekania przyrostowego

	Conventional alloys	Long-term cooling at a CTE of 14.5 µm/m·K and above		
	Paste opaque 1+2	Opaque dentine	Dentine	Glaze
Pre-heating, °C	575	575	575	575
Drying time, min	7:00	6:00	4:00	3:00
Heating rate, °C/min	55	55	55	55
Final temperature, °C	930	910	900	890
Holding time, min	2:00	1:00	1:00	1:00
Vacuum, hPa	50	50	50	-
Extended cooling	-	3 min/850°C	3 min/850°C	3 min/850°C

oxide layer. To ensure better contact between titanium biomaterial and ceramics, an intermediate layer - paste bonder - was used. Next, two opaque layers were used to eliminate the metallic colour and opaque dentin. The next sprayed layers of ceramics are dentin and enamel.

The set of discs made of glass ceramics (lithium disilicate) was veneered with low-melting nanofluoroapatite glass ceramics in the IPS e.max Ceram system. This ceramics was used due to the low firing temperature of 750ºC and the appropriate range of the thermal expansion coefficient of 9.5 µm/m·K. The following ceramic layers were fired: opaque dentin, dentin, and incisal. Incisal is a layer of transparent material used to obtain a high quality outer layer. Veneering of the glass-ceramic substructure with the applied system ensured aesthetic values and balance between brightness, chromaticity, and internal light scattering.

Zirconium oxide discs stabilized with yttrium oxide were veneered with the Elephant Sakura system. Zirconium oxide has the advantage that it is hard and very durable. It is also a light transmitting material. A transparency of approx. 50% enables natural-looking restorations to be made. Zirconium oxide is also semi-covering, which allows for aesthetic covering of discoloured tooth crowns. Prior to the firing procedures for the silica ceramic layers, the zirconium oxide discs were cleaned in a steam jet. One should not sandblast them, as this process can locally produce extremely high temperatures, which can damage the substructure. Standard layering technology is used for the firing of veneering ceramics. An opaque layer of liner was applied to the samples. Liner does not affect grip, but physically conditions the surface. It reduces the surface tension of the substructure. Then the value dentin layer was applied and fired. This material is grouped by colour and brightness level with a fluorescent effect. Then the enamel layers were sprayed: incisal and clear. Incisal is a transparent opalescent material used to obtain a high quality outer layer. Clear is a neutral, transparent layer that does not reflect on the incisal edge.

RESULTS

The analysis of stereometric images characterizing the tested surfaces indicates the regularity of the micrometric waves and their round shapes for all tested samples.

Microscopic images and graphs of surface roughness in the 3D height mode of samples veneered with Duceram Kiss ceramic on the CoCrMo substructure with milling technology and SLM technology have a uniform structure with gentle elevations and depressions, and with very few porosities **(Figs. 5** and **6)**. The maximum height of elevations for samples from milling technology is 6.3 µm and is smaller than for SLM technology for which the elevations reach the value of 13.6 µm. The mild roughness character of the samples is confirmed by sample profiles in selected areas on the surface of the samples **(Figs. 13a, b)**. Average roughnesses determined from profiles have the lowest values for veneering this ceramics on the basis of the milling technology **(Tab. 2)**. Duceram Kiss ceramics sprayed on CoCrMo samples with SLM has higher values of all roughness parameters.

Veneering of titanium with the Vita Titankeramik system resulted in different microscopic images and different roughness diagrams in 3D mode, depending on the substructure being used **(Figs. 7–9)**. The images and roughness diagrams veneered with this ceramics differed significantly from the microscopic images and 3D diagrams of roughness obtained by veneering on CoCrMo and glass ceramic and ceramic substructures **(Figs. 5, 6, 10,** and **11)**. Vita Titankeramik ceramics veneering of pure milled titanium and Ti6Al4V alloy from the milling technology is characterized by targeted structure with visible pores **(Figs. 7** and **8)**. Numerous pores occur on the TiCP substructure veneer surface, and single, but larger, on the veneering surface of the Ti6Al4V substructure from milling. In stereometric images of these surfaces, elevations and depressions "shred" the surface in a targeted manner, and the values of the elevations do not have large values: 9.6 µm for the TiCP substrate and 5.6 µm for the substrate with Ti6Al4V. 3D images generally differ from the other

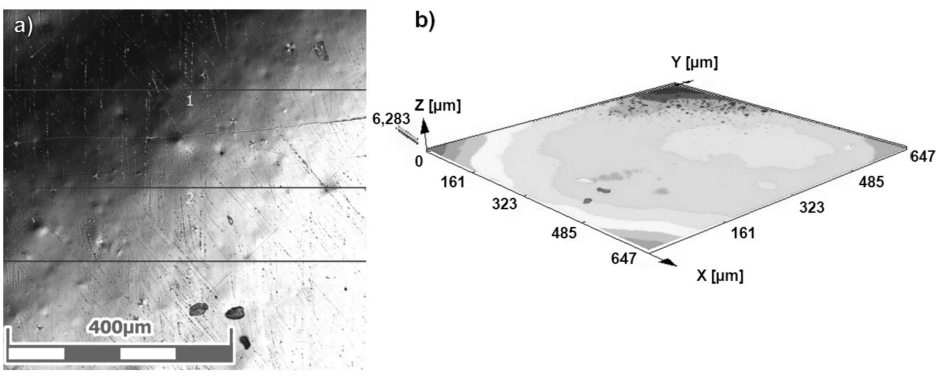

Fig. 5. Images of the surface veneered with Duceram Kiss ceramics on the CoCrMo milled substructure: a) 2D intensity mode, b) 3D height mode

Rys. 5. Obrazy powierzchni licowanej ceramiką Duceram Kiss na podbudowie CoCrMo frezowanej: a) tryb intensity 2D, b) tryb wysokości 3D

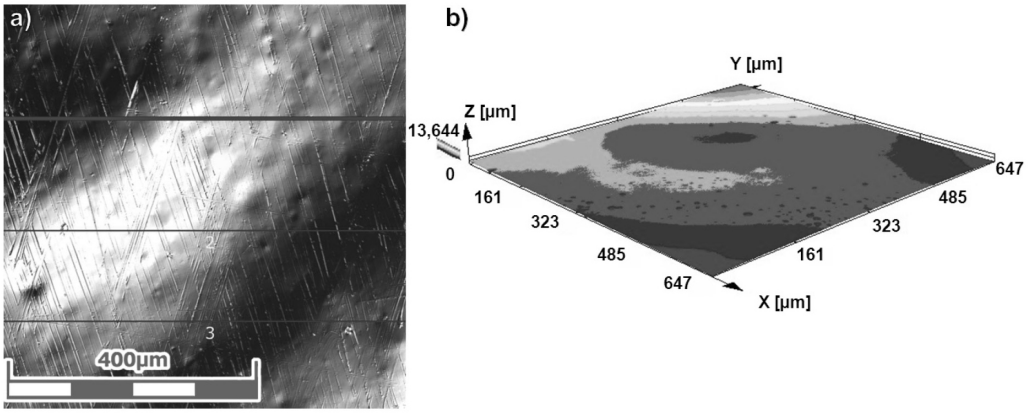

Fig. 6. Images of the surface veneered with Duceram Kiss ceramics on the CoCrMo substructure with incremental sintering: a) 2D intensity mode, b) 3D height mode

Rys. 6. Obrazy powierzchni licowanej ceramiką Duceram Kiss na podbudowie CoCrMo z przyrostowego spiekania: a) tryb intensity 2D, b) tryb wysokości 3D

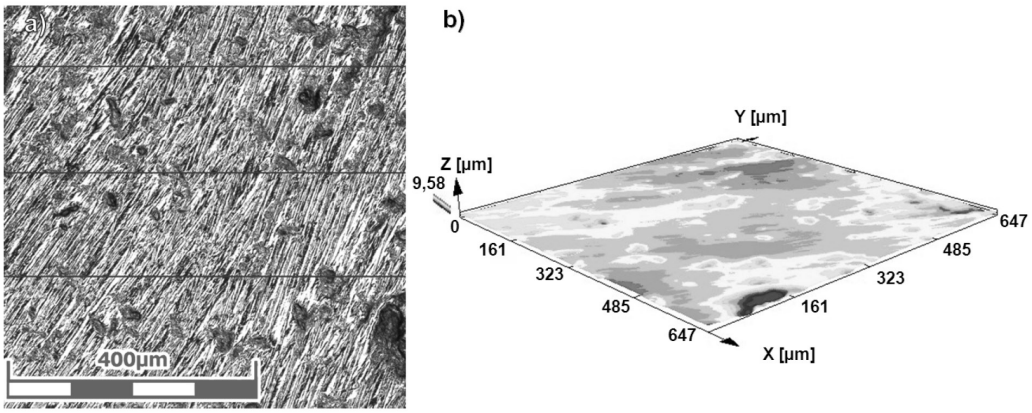

Fig. 7. Images of the surface veneered with Vita Titankeramik ceramics on the milled TiCP base: a) 2D intensity mode, b) 3D height mode

Rys. 7. Obrazy powierzchni licowanej ceramiką Vita Titankeramik na podbudowie TiCP frezowanej: a) tryb intensity 2D, b) tryb wysokości 3D

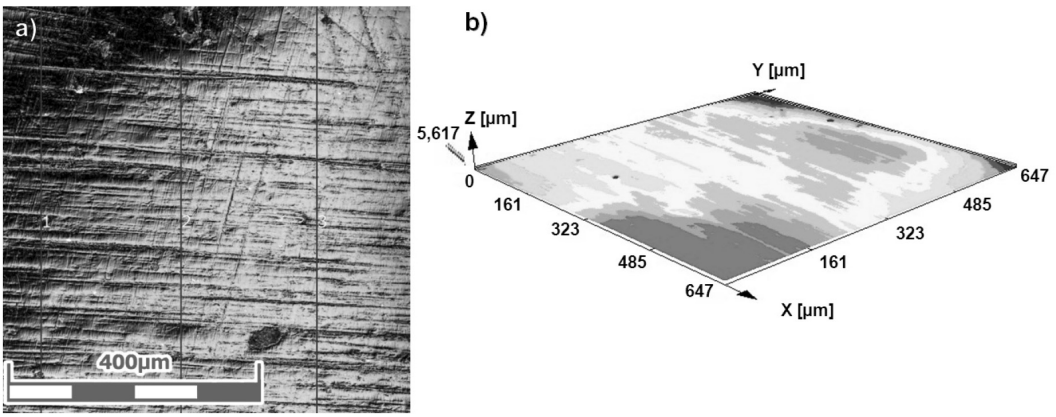

Fig. 8. Images of the surface veneered with Vita Titankeramik ceramics on the Ti6Al4V milled substructure: a) 2D intensity mode, b) 3D height mode

Rys. 8. Obrazy powierzchni licowanej ceramiką Vita Titankeramik na podbudowie Ti6Al4V frezowanej: a) tryb intensity 2D, b) tryb wysokości 3D

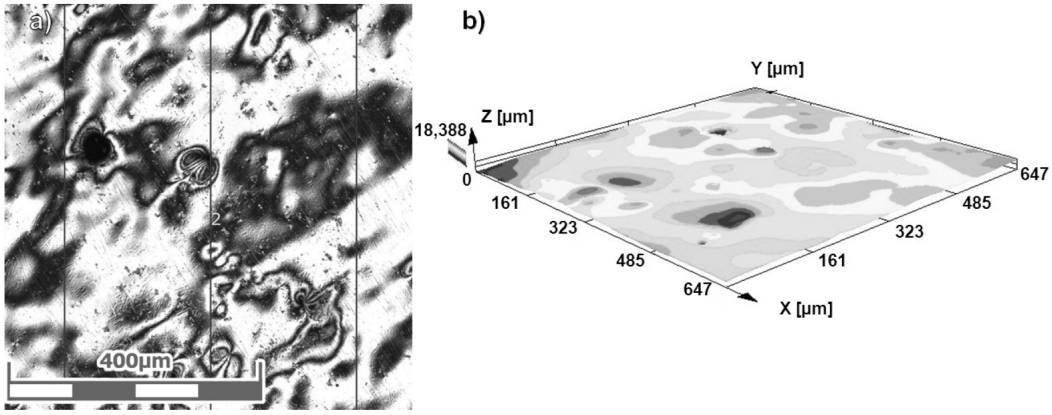

Fig. 9. Vita Titankeramik ceramic veneered with images on Ti6Al4V substructure with incremental sintering: a) 2D intensity mode, b) 3D height mode

Rys. 9. Obrazy powierzchni licowanej ceramiką Vita Titankeramik na podbudowie Ti6Al4V z przyrostowego spiekania: a) tryb intensity 2D, b) tryb wysokości 3D

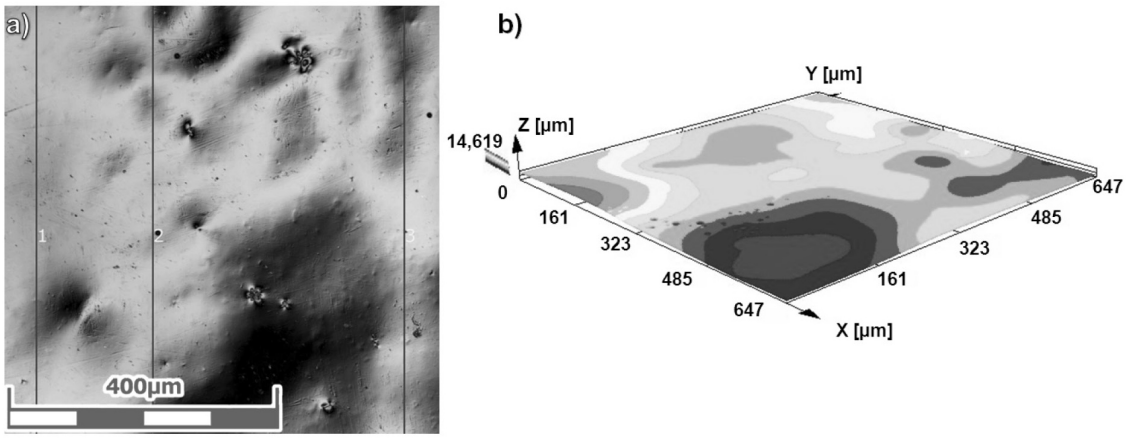

Fig. 10. IPS e.max Ceram veneered with on $LiSi_2$ milled substructure: a) 2D intensity mode, b) 3D height mode

Rys. 10. Obrazy powierzchni licowanej ceramiką IPS e.max Ceram na podbudowie $LiSi_2$ frezowanej: a) tryb intensity 2D, b) tryb wysokości 3D

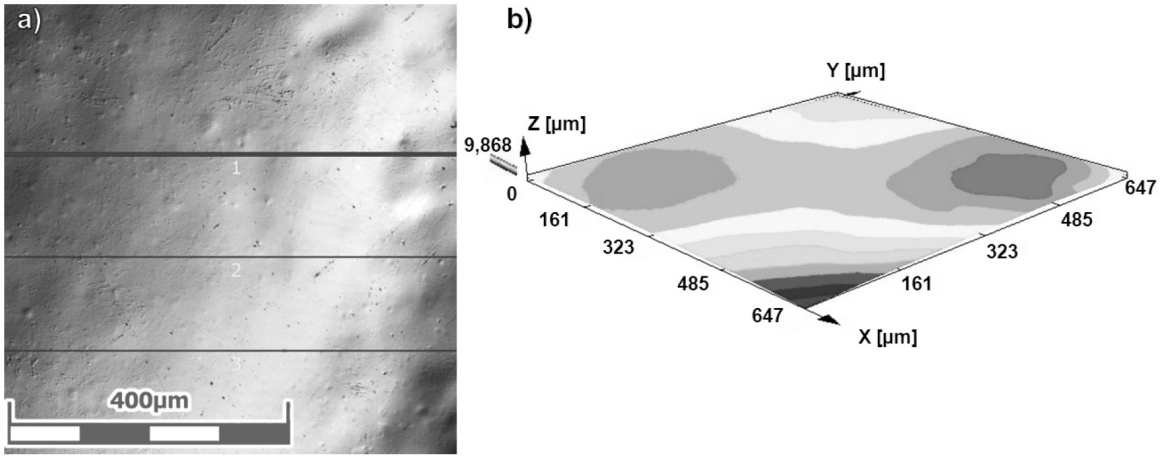

Fig. 11. Images of the surface veneered with Elephant Sakura ceramics on the milled ZrO_2 substructure: a) 2D intensity mode, b) 3D height mode

Rys. 11. Obrazy powierzchni licowanej ceramiką Elephant Sakura na podbudowie ZrO_2 frezowanej: a) tryb intensity 2D, b) tryb wysokości 3D

images from the tested veneering layers and enamel. It can be assumed that the visible furrow is the result of the difficult machinability of titanium and its alloys. These structures are confirmed by the linear profiles on the surface of the samples, which have numerous irregular folds **(Figs. 13c, d)**. Veneering with this ceramics of the Ti6Al4V substructure in SLM technology gives a picture of the structure different from that of the milled specimens, with a higher regularity of elevations and cavities **(Fig. 9)**. Large, round elevations with a maximum height of 18.4 µm, despite regular shapes, can accelerate wear, and, if they are very hard, damage the surface of the opposing tooth. They may also break out of the veneering layer. This regularity, large pores and oval protrusions and 3D dents are confirmed by the line graph, which has regular numerous folds with higher amplitude **(Fig.13e)**. In the case of titanium substructure, it can be said that the technology of its production affects the structure and character of the surface shape and its roughness.

The next test results concern the procedure of the veneering of the milled substructure made of factory-made glass blocks of silicone-lithium ceramics for which IPS e.max Ceram ceramics was used. The microscopic image and the roughness diagram in 3D height mode show a uniform structure with small porosity and very gentle waveforms with high amplitude and long duration **(Fig. 10)**. Maximum heights reach 14.6 µm. The very gentle wave character is confirmed by the roughness profile in the line **(Fig. 13f)**.

The most smooth and homogeneous surface was observed in the samples with milled and sintered zirconium substructures, which were veneered with Elephant Sakura silica ceramics **(Fig. 11)**. In 3D images, the heights reach 9.9 µm. The surface profile in the line is the most regular of all tested samples veneered with ceramics on different substructures **(Fig. 13g)**.

The shape of the top layer of the enamel was investigated as a reference surface. In the microscopic area the structure is uniform and regular **(Fig. 12)**. The roughness diagram in 3D mode shows a gentle, even wavelength that has the largest amplitudes of all tested samples. The elevation values reach a height of 152 µm. The roughness profile of the selected line **(Fig. 13h)** also shows mild undulations with the same long period of time.

Stereometric analysis based on isometric images **(Figs. 5b–12b)** characterizing the tested surfaces indicates the regularity of waviness and rounded shapes for all tested samples. They differ in absolute heights of elevations and depressions.

Average amplitude parameters were determined for the tested samples from the roughness profiles and are indicated in **Figures 5a–12a**: Ra – mean arithmetic deviation of the roughness profile, Rq – mean square deviation of the roughness profile, Rz – sum of heights for the highest elevation and depth of the lowest depression in the roughness profile, Rv – depth of the lowest depression in the roughness profile, Rp – height of the highest elevation of the roughness profile.

The average parameters of the roughness of veneered surfaces differ from each other **(Tab. 2)**. The smoothest veneering layers were obtained on the milled Duceram Kiss veneering substructure and on the milled and sintered zirconium base veneered with Elephant Sakura ceramics.

Veneering layers of milling technology substructures are characterized by lower values of roughness parameters, meaning that they are smoother than veneering layers of SLM substructures. This was the case for CoCrMo and titanium-based samples **(Tab. 2)**.

The highest roughness parameters were found in enamel examination from chewing surfaces and from the lateral surfaces of premolars and lateral teeth. All determined parameters were several times higher than the parameters of veneering layers.

It can be said that the average roughness parameters give worse information than the real image of the tested

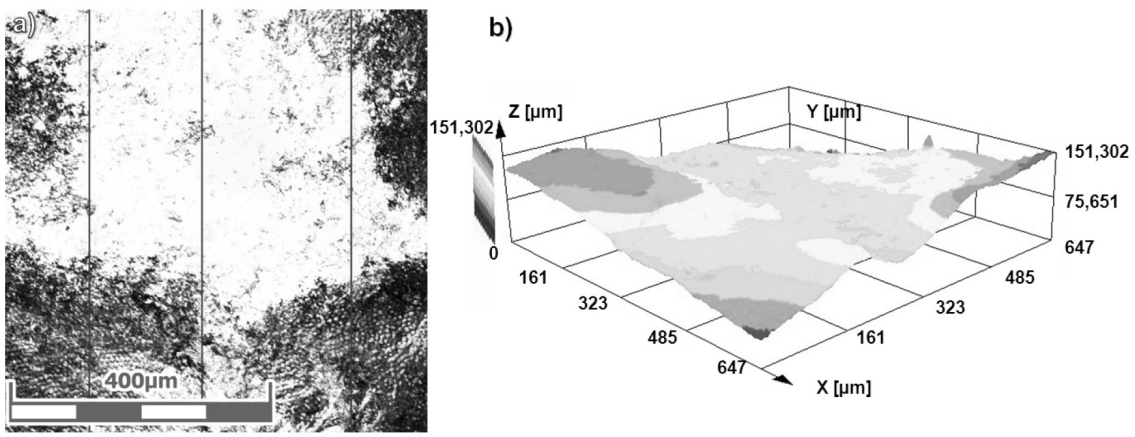

Fig. 12. Enamel surface images: a) 2D intensity mode, b) 3D height mode
Rys. 12. Obrazy powierzchni szkliwa: a) tryb intensity 2D, b) tryb wysokości 3D

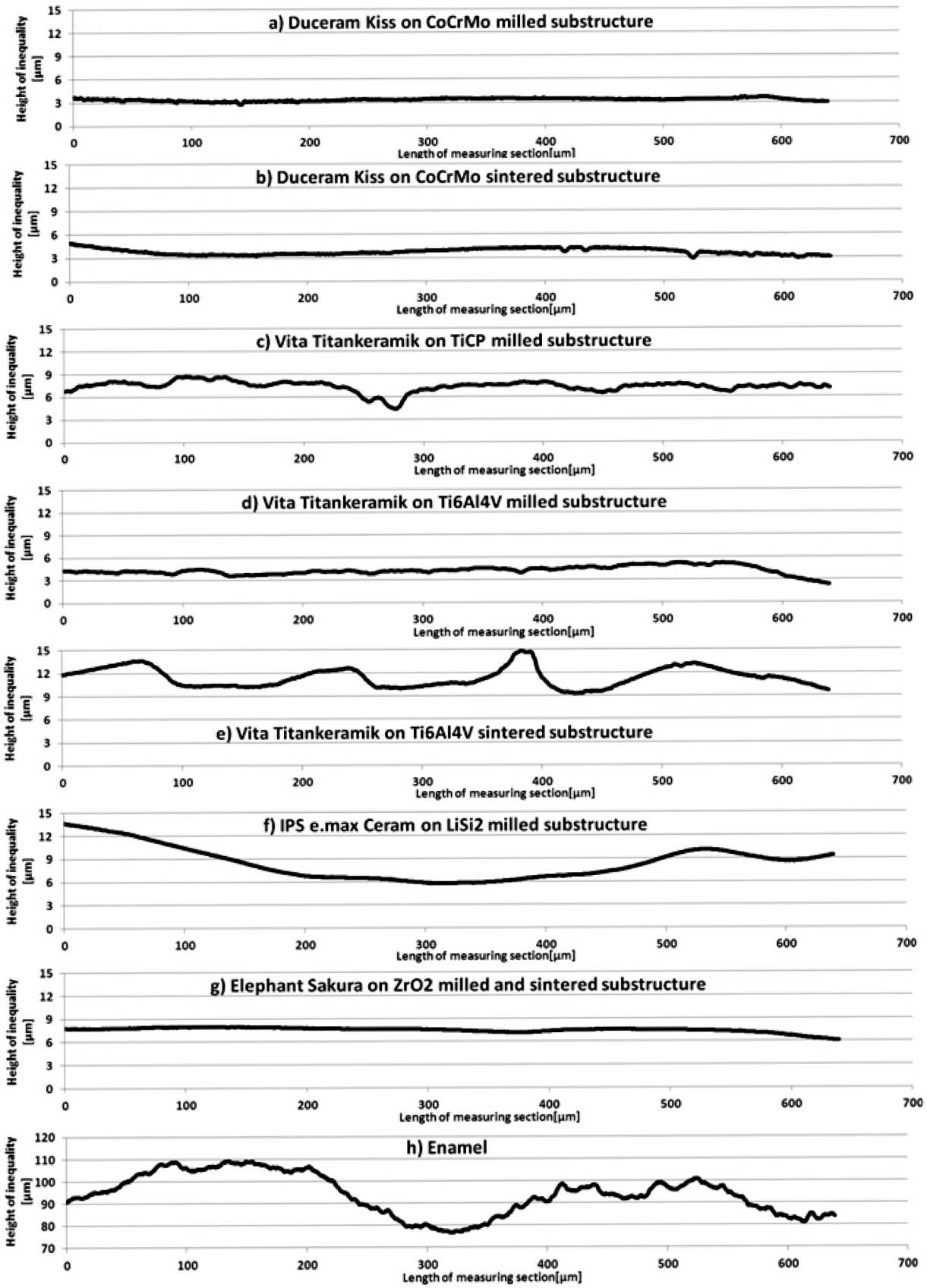

Fig. 13. List of profiles in the selected lines No. 2 (shown in Figs. 5a–12a) of the veneering surfaces of samples and enamel
Rys. 13. Zestawienie profili w wybranych liniach nr 2 (oznaczonych na **Rys. 5a–12a**) licowanych powierzchni próbek oraz szkliwa

Table 2. List of average values of roughness parameters from marked lines on the tested sample veneering surfaces according to ISO 4287

Tabela 2. Zestawienie średnich wartości parametrów chropowatości z oznaczonych linii na badanych powierzchniach licowania próbek wg ISO 4287

Material		Average values of roughness parameters [μm]				
The veneering layer	Substructure	**Ra**	**Rq**	**Rz**	**Rv**	**Rp**
Duceram Kiss	**CoCrMo - milling**	0.120	0.152	1.010	0.578	0.431
	CoCrMo - sintering	0.343	0.387	1.819	0,781	1.039
Vita Titankeramik	**TiCP - milling**	0.467	0.692	4.143	3.039	1.105
	Ti6Al4V - milling	0.352	0.520	2.967	2.068	0.899
	Ti6Al4V - sintering	2.393	2.878	10.066	5.690	4.376
IPS e.max Ceram	**$LiSi_2$ – milling**	1.830	2.019	6.704	2.667	4.037
Elephant Sakura	**ZrO_2 – milling and sintering**	0.168	0.225	1.178	0.864	0.314
Enamel		6,924	8.113	8.113	17.293	11.933

samples in which defects, fragments, and the impact of the top layer of the substructures resulting from the production technology are visible.

The stereometric image of the enamel top layer is characteristic. Elevations and depressions have much higher absolute values, but their nature is very regular and gentle. There are no discontinuities in the 2D image. With such images of biomaterial and enamel surfaces, it is necessary to explain the process of wear and resistance to displacement of such shaped surfaces by means of a tribological experiment.

DISCUSSION OF TEST RESULTS

Ceramic fillings are fired at a given temperature and time. The temperature increases at a steady rate until a certain level is reached, at which the temperature is maintained for a certain period of time until all reactions have been completed. An adequate rise in temperature is beneficial, because ceramics are poor conductors. Moreover excessively rapid heating can excessively melt the outer layers before the inner part is properly sintered.

A minimum of three firing procedures are required for the ceramic-metal filling: one for the opaque layer, one for the dentin and enamel layer, and one for the dyes and glaze. However, due to the shrinkage associated with the sintering process, it is necessary to layer ceramics with some excess. In a ceramic and metal filling, the basic condition is that the coefficients of thermal expansion of veneering ceramics are slightly smaller than that of metal **[L. 10, 15, 16]**. As a result, the ceramics are subjected to low compressive stresses during cooling, which ensure greater resistance to cracks and chipping. When veneering with ceramics, air bubbles are a problem, which form pores, which are visible on the images of veneering surfaces of samples **(Figs. 14c, d,** and **e)**.

Leaks are the result of air entrapment of during the sintering process. Under the influence of surface tension, air spaces become spherical and expand with increasing temperature. The examined ceramics veneering metal substructures were fired in a vacuum. After closing the furnace door, the pressure inside was reduced to 50 hPa, while the temperature increased until the melting point was reached. At that time, the vacuum was eliminated and the pressure in the furnace returned to 1000 hPa. The pressure increase from 50 to 1000 hPa helped compress and close the remaining pores. Despite this procedure, there were few residual specimens on the veneered surfaces of titanium-based milling and SLM specimens. Pores weaken the veneered surface and may be the focus of crack propagation. The veneering ceramics of milled zirconium substructures, and to lesser extent CoCrMo substructures from milling and SLM, were characterized by good surface structure quality and roughness parameters of small values **(Fig. 14)**. Lithium disilicate substructures veneered with nanofluoroapatite ceramics had proper surface structures with much higher roughness parameters.

The use of digital technologies, such as milling and SLM, to produce CAD/CAM substructures for prosthetics, has given rise to the need to assess the quality of veneering layers. Veneering of load-bearing structures with CoCrMo is the subject of works which evaluate the strength of bonds between veneering ceramics and the substructure **[L. 9]**, compare mechanical properties and strength of such a connection **[L. 10]**, and analyse the procedures of joining ceramics with CoCrMo alloy **[L. 17]**.

Veneering of load-bearing titanium structures from milling and SLM is a problem. This is indicated by the conducted studies and numerous reports in the literature in which the procedures of surface conditioning, alloy composition optimization, the chemical modification of the surface layer of the substructure, and the optimization of ceramics application and firing are sought **[L. 8, 18–23]**.

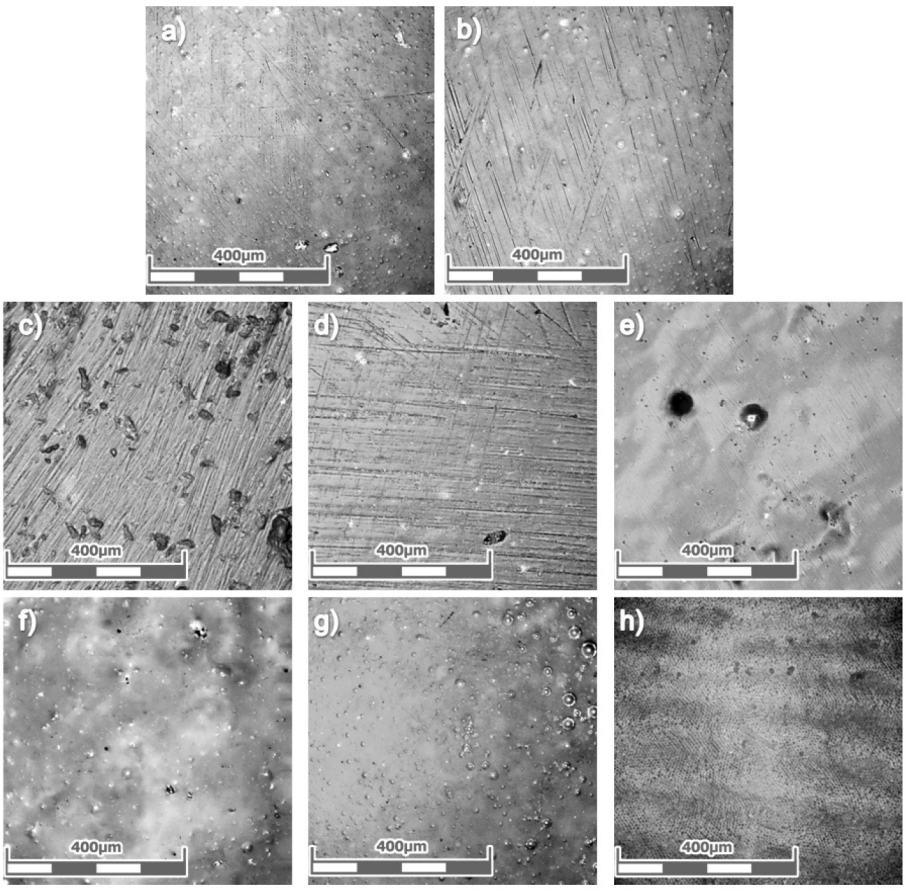

Fig. 14. Images of veneered surfaces of samples and enamel in 2D color mode: a) Duceram Kiss on CoCrMo milled substructure, b) Duceram Kiss on CoCrMo sintered substructure, c) Vita Titankeramik on TiCP milled substructure, d) Vita Titankeramik on Ti6Al4V milled substructure, e) Vita Titankeramik on Ti6Al4V sintered substructure, f) IPS e.max. Ceram on $LiSi_2$ milled substructure, g) Elephant Sakura on ZrO_2 milled and sintered substructure, h) Enamel

Rys. 14. Obrazy licowanych powierzchni próbek oraz szkliwa w trybie color 2D: a) Duceram Kiss na podbudowie CoCrMo frezowanej, b) Duceram Kiss na podbudowie CoCrMo spiekanej, c) Vita Titankeramik na podbudowie TiCP frezowanej, d) Vita Titankeramik na podbudowie Ti6Al4V frezowanej, e) Vita Titankeramik na podbudowie Ti6Al4V spiekanej, f) IPS e.max Ceram na podbudowie $LiSi_2$ frezowanej, g) Elephant Sakura na podbudowie ZrO_2 frezowanej i synteryzowanej, h) szkliwo

The evaluation of the veneering of the milled zirconium base is the subject of many study works. The authors analyse the adhesion of veneering ceramics to zirconium base **[L. 24–26]**, the quality of veneering with various types of modified ceramics and modified surfaces of the substructure **[L. 7, 27, 28]**, shear strength of the veneering layer **[L. 6, 29]** and the effect of mismatch of thermal expansion coefficients on the formation of residual stresses in veneering layers **[L. 30]**.

Few studies are devoted to the comparison of veneering ceramics in terms of tribological behaviour **[L. 6, 7, 24, 27, 29]**. According to the aim of the work, the tribological processes will be largely determined by the microgeometry of the surface and the structure of ceramics veneering the supporting substructures.

The examined enamel surfaces are characterized by a gentle profile with a high amplitude and a long period of time. The results of studies on the shape of the enamel surface with the use of AFM confirm the character of the surface layer stereometry **[L. 31–34]**. Considerations in terms of tribological processes in contact with saliva indicate an optimal lubrication mechanism due to the shape of the enamel surface. Over the course of this mechanism, lubricating micro- and nano-wedges filled with saliva, which protect the cooperating tooth surfaces under occlusion and chewing conditions, are significant. The process of the moistening of the top layer of the enamel by saliva should be considered, which creates a permanent lubricating film. Active enzymes present in saliva affect the film structure. The parameters of the enamel roughness differ significantly from the parameters of veneering ceramics. Prisms are the basic element of the enamel structure and they determine its resistance. They run perpendicularly from the enamel-teeth connection to the surface of the tooth crown. On the crown surface, they form an arcaded articulatory

surface. Their length ranges from several dozen to 2500 μm, while their width ranges from 5–9 μm. The length of the prism varies depending on the area of the tooth in which it is located. The maximum length occurs in the cusps, which carry the load in direct contact with the opposite teeth.

CONCLUSIONS

The roughness parameters of the veneered surfaces differ from each other. The smoothest veneering layers were obtained on the milled Duceram Kiss veneering substructure and on the milled and sintered zirconium base veneered with Elephant Sakura ceramics.

Veneering layers of milling technology substructures are characterized by lower values of roughness parameters, which indicates that they are smoother than veneering layers of SLM substructures. This regularity occurred for samples with substructures from CoCrMo and for samples with titanium substructures.

When comparing the top layers on titanium substructures from milling, on SLM substructures, it can be seen that objective information gives a real 3D image of the tested samples in which defects, fragments, and the impact of the technology of producing the top layer of the substructure are visible.

In case of the most perfect material, which currently is zirconium oxide stabilized with yttrium, we are unable to replicate strength, structural, aesthetic and wear resistance parameters resulting from the internal structure and shape of the top layer of the enamel **[L. 33, 34]**.

According to the aim of the work, the tribological processes will be largely determined by the microgeometry of the surface and the structure of ceramics veneering the supporting substructures. It should be examined whether cooperation of very smooth surfaces will be more beneficial for tribological contact in the presence of saliva, or whether it should be strived to obtain, in top layers, surfaces with regular spatial elevations and depressions.

ACKNOWLEDGEMENT

This work is financed by AGH University of Science and Technology, Faculty of Mechanical Engineering and Robotics: subvention No. 16.16.130.942 and a research project No. 2019/K/ZDS/006974 of Jagiellonian University Medical College, Poland.

REFERENCES

1. Malara P., Paluch K., Sobolewska K., Pasieka A.: The study of the connection between the zirconia substructure and veneering porcelain in dental crowns subjected to occlusal forces. Archives of Materials Science, 6(2016), 6.
2. Toussi C.A., Ezatpour H.R., Haddadnia J., Shiri J.G.: Effect of using different metal and ceramic materials as restorations on stress distribution around dental implants: a comparative finite element study. Materials Research Express, 5, 11(2018), pp. 115403.
3. Malara P., Paluch K., Sobolewska K., Pasieka A.: Assessment of the compressive strength of the metal-ceramic connections in fixed dental restorations. Journal of Achievements in Materials and Manufacturing Engineering, 79, 2(2016), pp. 66–73.
4. Ryniewicz W., Ryniewicz A.M.: Analiza modelowa układu stomatognatycznego przy odbudowach z zastosowaniem mostów protetycznych. Przegląd Elektrotechniczny, 91, 5(2015), pp. 17–20.
5. Bojko Ł., Ryniewicz W., Ryniewicz A.M., Kot M., Pałka P.: The influence of additive technology on the quality of the surface layer and the strength structure of prosthetic crowns. Tribologia, 4(2018), pp. 13–22.
6. Zaher A.M., Hochstedler J.L., Rueggeberg F.A., Kee E.L.: Shear bond strength of zirconia-based ceramics veneered with 2 different techniques. The Journal of prosthetic dentistry, 118, 2(2017), pp. 221–227.
7. Kirmali O., Kapdan A., Kustarci A., Er K.: Veneer ceramic to Y-TZP bonding: comparison of different surface treatments. Journal of Prosthodontics, 25, 4(2016), pp. 324–329.
8. Fukuyama T., Hamano N., Ino S.: Effects of silica-coating on surface topography and bond strength of porcelain fused to CAD/CAM pure titanium. Dental materials journal, 35, 2(2016), pp. 325–332.
9. Bae E.J., Kim H.Y., Kim W.C., Kim J.H.: In vitro evaluation of the bond strength between various ceramics and cobalt-chromium alloy fabricated by selective laser sintering. The journal of advanced prosthodontics, 7, 4(2015), pp. 312–316.
10. Han X., Sawada T., Schille C., Schweizer E., Scheideler L., Geis-Gerstorfer J., Spintzyk S.: Comparative analysis of mechanical properties and metal-ceramic bond strength of Co-Cr dental alloy fabricated by different manufacturing processes. Materials, 11, 10(2018), p. 1801.
11. Ryniewicz W., Ryniewicz A.M., Bojko Ł.: The effect of a prosthetic crown's design on the accuracy of mapping an abutment teeth's shape. Measurement, 91(2016), pp. 620–627.
12. Ryniewicz A.M., Bojko Ł., Ryniewicz W.I.: Microstructural and micromechanical tests of titanium biomaterials intended for prosthetic reconstructions. Acta of bioengineering and biomechanics, 18, 1(2016), pp. 121–127.

13. Nguyen H.H., Wan S., Tieu K.A., Pham S.T., Zhu, H.: Tribological behaviour of enamel coatings. Wear, 426(2019), pp. 319–329.
14. Sinthuprasirt P., van Noort R., Moorehead R., Pollington S.: Evaluation of a novel multiple phase veneering ceramic.Dental Materials, 31, 4(2015), pp. 443–452.
15. Papia E., Arnoldsson P., Baudinova A., Jimbo R., Von Steyern P.V.: Cast, milled and EBM-manufactured titanium, differences in porcelain shear bond strength. Dental materials journal, 37, 2(2018), pp. 214–221.
16. Sakaguchi R.L., Powers J.M.: Craig's restorative dental materials. Elsevier Health Sciences, Philadelphia 2012.
17. Antanasova M., Kocjan A., Kovač J., Žužek B., Jevnikar P.: Influence of thermo-mechanical cycling on porcelain bonding to cobalt–chromium and titanium dental alloys fabricated by casting, milling, and selective laser melting. Journal of prosthodontic research, 62, 2(2018), pp. 184–194.
18. Yang J., Kelly J.R., Bailey O., Fischman G.: Porcelain-titanium bonding with a newly introduced, commercially available system. The Journal of prosthetic dentistry, 116, 1(2016), pp. 98–101.
19. Guilherme N., Wadhwani C., Zheng C., Chung K.H.: Effect of surface treatments on titanium alloy bonding to lithium disilicate glass-ceramics. The Journal of prosthetic dentistry, 116, 5(2016), pp. 797–802.
20. Antanasova M., Jevnikar P.: Bonding of dental ceramics to titanium: processing and conditioning aspects.Current Oral Health Reports, 3, 3(2016), pp. 234–243.
21. Sendao I.A., Alves A.C., Galo R., Toptan F., Silva F.S., Ariza E.: The effect of thermal cycling on the shear bond strength of porcelain/Ti–6Al–4V interfaces. Journal of the mechanical behavior of biomedical materials, 44(2015), pp. 156–163.
22. Parchańska-Kowalik M., Wołowiec-Korecka E., Klimek L.: Effect of chemical surface treatment of titanium on its bond with dental ceramics. The Journal of prosthetic dentistry, 120, 3(2018), pp. 470–475.
23. Golebiowski M., Wolowiec E., Klimek L.: Airborne-particle abrasion parameters on the quality of titanium-ceramic bonds. The Journal of prosthetic dentistry, 113, 5(2015), pp. 453–459.
24. Qi G., Huiqiang S., Yijun H., Jia C., Weishan D.: Effect of different surface processes on the bond strength between zirconia framework and veneering ceramic. Hua xi kou qiang yi xue za zhi= Huaxi kouqiang yixue zazhi= West China journal of stomatology, 35, 6(2017), pp. 598–602.
25. Kanat-Ertürk B., Çömlekoğlu E.M., Dündar-Çömlekoğlu M., Özcan M., Güngör M.A.; Effect of veneering methods on zirconia framework—Veneer ceramic adhesion and fracture resistance of single crowns. Journal of Prosthodontics, 24, 8(2015), pp. 620–628.
26. Gautam C., Joyner J., Gautam A., Rao J., Vajtai R.: Zirconia based dental ceramics: structure, mechanical properties, biocompatibility and applications. Dalton Transactions, 45, 48(2016), pp. 19194–19215.
27. Grohmann P., Bindl A., Hämmerle C., Mehl A., Sailer I.: Three-unit posterior zirconia-ceramic fixed dental prostheses (FDPs) veneered with layered and milled (CAD-on) veneering ceramics: 1-year follow-up of a randomized controlled clinical trial. Quintessence International, 46, 10(2015), pp. 871–880.
28. Pharr S.W., Teixeira E.C., Verrett R., Piascik J.R.: Influence of Veneering Fabrication Techniques and Gas-Phase Fluorination on Bond Strength between Zirconia and Veneering Ceramics. Journal of Prosthodontics, 25, 6(2016), pp. 478–484.
29. Craciunescu E., Sinescu C., Negrutiu M.L., Pop D.M., Lauer H.C., Rominu M., Antoniac I.: Shear bond strength tests of zirconia veneering ceramics after chipping repair. Journal of adhesion science and Technology, 30, 6(2016), pp. 666–676.
30. Mainjot A.K., Najjar A., Jakubowicz-Kohen B.D., Sadoun M.J.: Influence of thermal expansion mismatch on residual stress profile in veneering ceramic layered on zirconia: Measurement by hole-drilling. Dental Materials, 31, 9(2015), pp. 1142–1149.
31. Ryniewicz W., Herman M., Ryniewicz A.M., Bojko Ł., Pałka P., Ryniewicz A., Madej T.: Tribological tests of the nanomaterials used to reconstruct molars and premolars with the application of the direct method. Tribologia, 3(2017), pp. 155–164.
32. Ryniewicz W., Herman M., Ryniewicz A.M., Bojko Ł., Pałka P.: Tribological Tests of Nanocomposites for Direct Restoration of Teeth. Tribologia, 4(2018), pp. 97–105.
33. Herman M., Ryniewicz A.M., Ryniewicz W.: The analysis of determining factors of enamel resistance to wear. Pt. 1, Identification of biological and mechanical enamel structure and its shape in dental crowns. Engineering of Biomaterials, 13, 95(2010), pp. 10–17.
34. Ryniewicz W., Herman M., Ryniewicz A.M.: The analysis of enamel resistance to wear determining factors. Pt. 2, Study of superficial layer and microhardness in tooth enamel. Engineering of Biomaterials, 14, 102(2011), pp. 23–27.